J|A|C|S ARTICLES

Published on Web 09/17/2009

First Principles Modeling of Eosin-Loaded ZnO Films: A Step toward the Understanding of Dye-Sensitized Solar Cell Performances

Frédéric Labat,[†] Ilaria Ciofini,[†] Hrant P. Hratchian,[‡] Mike Frisch,[‡] Krishnan Raghavachari,[§] and Carlo Adamo[†,*]

Laboratoire d'Electrochimie, Chimie des Interfaces et Modélisation pour l'Energie, CNRS UMR-7575, Ecole Nationale Supérieure de Chimie de Paris, 11 rue P. et M. Curie, F-75231 Paris Cedex 05 France, Gaussian, Inc., 340 Quinnipiac Street, Building 40, Wallingford, Connecticut 06492, and Department of Chemistry, Indiana University, Bloomington, Indiana 47405

Received April 20, 2009; E-mail: carlo-adamo@enscp.fr

Abstract: A theoretical investigation of eosin-Y (EY) loaded ZnO thin films, the basic components of a dye-sensitized solar cell (DSSC), is presented. The EY/ZnO wurtzite (10−10) system has been fully described within a periodic approach using density functional theory (DFT) and a hybrid exchange-correlation functional. Reduced systems were also analyzed to simulate an electron transfer from the dye to the substrate. Injection times from dye to the semiconductor were calculated using the Newns−Anderson approach. Finally, the UV−visible spectra of EY/ZnO films were simulated using a time-dependent DFT approach and compared to that of the EY molecule computed in solution. The results obtained highlight that EY strongly adsorbs on the ZnO substrate contributing significantly to the electronic structure of the adsorbed system. The UV−visible spectral signature of the isolated EY molecule is still found when adsorbed on ZnO but the analysis of Γ-point crystalline orbitals reveals that a direct HOMO→LUMO excitation cannot lead to a direct electron injection into the semiconductor, the first unoccupied orbital with contributions from the ZnO substrate being the LUMO + 1. As a consequence, a two photon injection mechanism is proposed explaining the low efficiency of the EY/ZnO solar cells. On this basis, possible strategies for enhancing the cell efficiency are presented and discussed.

1. Introduction

Within the global challenge for sustainable development of renewable energy sources, photovoltaic technologies play a major role, combining nontoxic to noise-free and low greenhouse gas emissions operations. While an intensive research has been successfully performed at the laboratory scale (multijunction solar cells have, for example, very recently achieved over 40% conversion efficiency[1]), high cost is the main parameter still limiting the implementation of solar electricity to a very large scale.[2] Among the possibilities investigated to cut costs, organic molecules and polymers are two of the most explored alternatives. Both classes of systems also present pleasing advantages over traditional inorganic compounds, such as flexibility and easier spectral tunability. In particular, introduction of thin film technologies led to the development of the so-called "dye-sensitized solar cells" (DSSC) in the early 1990s,[3] which perform with some remarkable analogies to the natural process of photosynthesis, shifting the optical response of a large band gap semiconductor (typically TiO_2) from the UV to the visible by dye sensitization.[4] In the commonly accepted model, upon light absorption, the dye is promoted into an excited state from where an ultrafast electron injection process takes place into the conduction band of the semiconductor (Figure 1a). Regeneration of the dye as well as diffusion of the charge carriers is ensured by both the presence of a redox couple in the electrolyte and suitable energy band positioning, loss mechanisms being largely suppressed by a favorable kinetic balance (see ref 5 for instance for a more detailed description of DSSC operating principles).

Like in plants, where an absorption enhancement is achieved by stacking the chlorophyll-containing thylakoid membranes of the chloroplast to form the grana structures,[6] a key to the high efficiency of these cells relies on the use of a porous film consisting of nanometer-sized semiconductor particles, allowing for nearly quantitative light harvesting over a broad range of the dye absorption spectrum with only a dye monolayer on each particle,[5] due to the 1000-fold enhancement of the effective surface area in this configuration. In addition, in these cells, absorption and electron transport processes are separated, and respectively carried out by the dye and the semiconductor, thus

[†] ENSCP.
[‡] Gaussian Inc.
[§] Indiana University.

(1) King, R. R.; Law, D. C.; Edmondson, K. M.; Fetzer, C. M.; Kinsey, G. S.; Yoon, H.; Krut, D.D.; Hermer, J. H.; Sherif, R. A.; Karam, N. H. *Adv. Optoelectron.* **2007**, Article ID 29523.
(2) Goetzberger, A.; Hebling, C. *Sol. Energy Mater. Sol. Cells* **2000**, *62*, 1.
(3) O'Regan, B.; Grätzel, M. *Nature* **1991**, *353*, 737.
(4) Lenzmann, F. O.; Kroon, J. M. *Adv. Optoelectron.* **2007**, Article ID 65073.
(5) Kalyanasundaram, K.; Grätzel, M. *Coord. Chem. Rev.* **1998**, *177*, 347.
(6) Kay, A.; Grätzel, M. *J. Phys. Chem.* **1993**, *97*, 6272.

10.1021/ja902833s CCC: $40.75

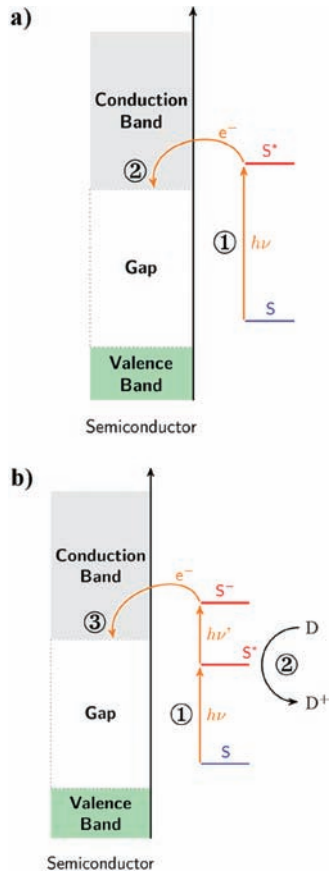

Figure 1. Sketches of the electron injection mechanisms in dye-sensitized solar cells: (a) injection from the dye excited state, (b) injection from the dye reduced state (D is an electron donor).

providing a higher tolerance for impurities compared to traditional inorganic photovoltaic modules.

Today, the most efficient DSSCs are based on polypyridyl−metal complexes such as the so-called N3 dye (cis-[Ru(4,4′-COOH-2,2′-bpy)$_2$(NCS)$_2$]), chemically bound to the anatase TiO_2 nanoparticles by designated carboxylated anchor groups. So far, with sizes around 1 cm^2, the best devices have reached around 11% conversion efficiency under standard test conditions.[7] Although extensive fundamental and applied investigations have been carried out, substantial progress is still required in order to reach higher efficiencies, even if this technology is now beginning to be industrially applied.[4]

Photoactive materials in DSSCs are typically prepared by stepwise processing: formation of porous films of inorganic semiconductors by colloid coating and heat treatment (around 450 °C) followed by dye adsorption, by dipping the film in the dye solution.[8] Two main drawbacks of this colloidal process can be evidenced: (i) an active control of the crystallographic structure and pore sizes of the inorganic phase is difficult, resulting in electron traps and resistance to the electron percolation;[9] (ii) the heat treatment limits the substrate choice to heat-resistant materials, thus excluding temperature-sensitive materials, such as polymers.

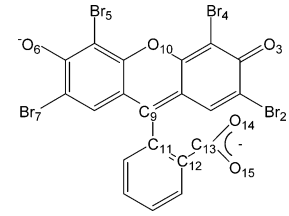

Figure 2. Sketches and atom labeling of the eosin-Y dianion, EY.

Recently however, a one-step low-temperature cathodic electrodeposition of dye-modified ZnO films process, which combines ease of preparation and high dye loading due to high porosity of the film,[8,9] has been proposed.[10,11] Among the successfully adsorbed dyes on ZnO thin films by such a method, tetrasulfonated metallophthalocyanines,[12,13] tetrabromophenol blue,[14] riboflavin 5 phosphate,[15] N3,[16,17] D149[18] or eosin-Y (2′,4′,5′,7′-tetrabromofluorescein, hereafter referred to as EY, see Figure 2)[8,19,20] are to be cited. Notably, the two latter dyes are part of a recent development trend devoted to purely organic dyes, mostly driven by potential lower costs (EY, for instance, is 1000 times cheaper than N3 dye[21]) and easier recycling of metal-free dye-based cells. An increasingly good photovoltaic performance, now very close to the best metal-based cells, has been reported (see ref 22 for some comments on this point) for such systems.

Electrochemically self-assembled EY/ZnO are characterized by high electron collection efficiency, better electron transport properties in the electrodeposited films than their colloidal counterparts[9] and automatic formation of the desired porous structure of the film by hindering of the crystal growth of ZnO.[8] Such process is particularly appealing from an experimental point of view, because it does not involve high temperatures, high mechanical stress, or aggressive chemicals, therefore being environmentally friendly and compatible with conductive plastic film substrates.[23] Unfortunately, EY/ZnO films have shown surprising low conversion efficiencies so far (max 2.3%),[9] and this overall low performance is yet to be understood.

In such a context, theoretical studies can provide valuable information on the first elementary steps of the DSSC mechanism, as well as on their tuning by the chemical environment.

(7) Green, M. A.; Emery, K.; King, D. L.; Hishikawa, Y.; Warta, W. *Prog. Photolvolaics* **2006**, *14*, 455.
(8) (a) Yoshida, T.; Terada, K.; Schlettwein, D.; Oekermann, T.; Sugiura, T.; Minoura, H. *Adv. Mater.* **2000**, *12*, 1214. (b) Terada, K.; Yoshida, T.; Sugiura, T.; Minoura, H. *Proc. 4th Int. Conf. Ecomater.* **1999**, 559.
(9) Oekermann, T.; Yoshida, T.; Minoura, H.; Wijayantha, K. G. U.; Peter, L. M. *J. Phys. Chem. B* **2004**, *108*, 8364.
(10) Yoshida, T.; Minoura, H. *Adv. Mater.* **2000**, *12*, 1219.
(11) Yoshida, T.; Pauporté, T.; Lincot, D.; Oekermann, T.; Minoura, H. *J. Electrochem. Soc.* **2003**, *150*, C608.
(12) Yoshida, T.; Miyamoto, K.; Hibi, N.; Sugiura, T.; Minoura, H.; Schlettwein, D.; Oekermann, T.; Schneider, G.; Wäohrle, D. *Chem. Lett.* **1998**, *27*, 599.
(13) Yoshida, T.; Tochimoto, M.; Schlettwein, D.; Wöhrle, D.; Sugiura, T.; Minoura, H. *Chem. Mater.* **1999**, *11*, 2657.
(14) Yoshida, T.; Yoshimura, J.; Matsui, M.; Sugiura, T.; Minoura, H. *Trans. Mater. Res. Soc. Jpn.* **1999**, *24*, 497.
(15) Karuppuchamy, S.; Yoshida, T.; Sugiura, T.; Minoura, H. *Trans. Mater. Res. Soc. Jpn.* **2001**, *397*, 63.
(16) Karuppuchamy, S.; Nonomura, K.; Yoshida, T.; Sugiura, T.; Minoura, H. *Solid State Ionics* **2002**, *151*, 19.
(17) Nonomura, K.; Yoshida, T.; Schlettwein, D.; Minoura, H. *Electrochim. Acta* **2003**, *48*, 3071.
(18) Minoura, H.; Yoshida, T. *Electrochemistry* **2008**, *76*, 109.
(19) Goux, A.; Pauporté, T.; Lincot, D.; Dunsch, L. *Chem. Phys. Chem.* **2007**, *8*, 926.
(20) Yoshida, T.; Oekermann, T.; Okabe, K.; Schlettwein, D.; Funabiki, K.; Minoura, H. *Electrochemistry* **2002**, *70*, 470.
(21) Suri, P.; Panwar, M.; Mehra, R. M. *Mater. Sci.* **2007**, *25*, 137.
(22) Kong, S.-Y.; Dai, Wang, K.-J. *Adv. Optoelectron.* **2007**, Article ID 75384.
(23) Yoshida, T.; Iwaya, M.; Ando, H.; Oekermann, T.; Nonomura, K.; Schlettwein, D.; Wöhrle, D.; Minoura, H. *Chem. Commun.* **2004**, *4*, 400.

Several papers have been recently devoted to atomistic simulation of DSSC. Accurate first-principles calculations, based on Density Functional Theory (DFT) and its extension to excited states (Time-Dependent DFT, TD-DFT) have been used for the simulation of spectral properties of isolated dyes (in gas phase or solvated) and their interactions with the redox mediator.[24−31] However, only a few papers have been devoted to the study of the dye/semiconductor interactions, most of them being limited to systems composed by TiO_2 and N3 or (smaller) model organic dyes.[32−39]

Despite the existing limitations of such simulations, mainly related to the chosen computational protocol (e.g., choice of the DFT approach) or to system modeling (cluster vs periodic systems), such theoretical studies have well underlined the valuable insights given by reliable theoretical approaches and their role in improving DSSC performances.

In line with these results, in this paper we give a detailed investigation of the EY/ZnO assembly, the core of a very promising hybrid photovoltaic system. Our aim is to describe the physicochemical properties of this assembly, which have not been theoretically studied to date, and to analyze how these properties control the observed (low) light conversion efficiency. To this end, a fully periodic DFT approach will be used to have a detailed and reliable description of the electronic (band structure) and structural properties of EY on the ZnO surface. Furthermore, some insights on the in situ spectral properties of EY and injection mechanism will be given, using a cluster model for the description of the excited state properties and a simple, but physically sound, model to compute the electron injection rate.

The core of our approach relies on different DFT tools that have been developed by our group during the last years that allow for an accurate treatment of electronic and spectroscopic properties in different phases (gas, solution, or solids). In particular, our approach provides accurate results for all the basic components of typical DSSC (dyes, semiconductor surfaces as well as combined dye/semiconductor systems[24,40−44]).

2. Computational Details

All periodic calculations have been carried out with the Crystal 03 code[45] which allows, using a localized (Gaussian) basis approach, to self-consistently solve both the Hartree−Fock (HF) and Kohn−Sham (KS) models as well as to use hybrid HF/KS methods. Throughout this paper, the PBE0 hybrid functional,[46,47] mixing 25% of HF exchange in a PBE scheme,[48] has been used.

All-electron basis sets, with (621/21/1), (8411/411/1), and (511/1) contractions for C, O, and H atoms, respectively, have been used for the adsorbate molecule (EY), Br atoms being described by large core Hay−Wadt pseudopotentials,[49] associated with a (31/31) valence basis set. Large core Durand−Barthelat pseudopotentials[50−52] with (31/31) valence basis set have been used for the O atoms of the ZnO substrate, while large core Hay−Wadt pseudopotentials[53] with (111/111/41) contractions have been considered for all Zn atoms. Such basis sets, whose s, p, and d polarization function exponents have been optimized using energy criteria, provide an accurate description of the electronic and structural parameters of both bulk and surfaces of ZnO.[54]

A large rectangular supercell, consisting of 128 atoms in a (4×4) supercell with dimensions of 13.3 Å and 20.7 Å in the periodic [1−210] and [000−1] directions, respectively, and 4 atomic planes in the nonperiodic [10−10] direction, has been used throughout. The irreducible Brillouin zone of the system is sampled with only one **k** point (Γ).[54] This supercell correctly mimics the ZnO substrate, since four atomic layers have been found sufficient for computational studies of surface adsorption on this substrate.[54−57] The final EY/ZnO unit cell has only one symmetry operator and is composed of 165 atoms, for a total of 4526 uncontracted primitive Gaussian functions.

To test if the formation of a surface dipole upon asymmetric adsorption of EY only on one side of the slab could induce some artifacts in the computed electronic structures of the native and charged systems, the same calculations were also performed with EY (and the corresponding acidic protons) symmetrically adsorbed on both slabs' surfaces. The results obtained are reported in the Supporting Information. The same conclusions hold (both from a qualitative and quantitative point of view) when using an asymmetric (one side, discussed hereafter) or symmetric (two sides) adsorption model, thus validating the model used and confirming the small role of surface dipole in such a system.

(24) Guillemoles, J. F.; Barone, V.; Joubert, L.; Adamo, C. *J. Phys. Chem. A* **2002**, *106*, 11354.
(25) De Angelis, F.; Tilocca, A.; Selloni, A. *J. Am. Chem. Soc.* **2004**, *126*, 15024.
(26) Labat, F.; Lainé, P. P.; Ciofini, I.; Adamo, C. *Chem. Phys. Lett.* **2006**, *417*, 445.
(27) Rekhis, M.; Labat, F.; Ouamerali, O.; Ciofini, I.; Adamo, C. *J. Phys. Chem. A* **2007**, *111*, 13106.
(28) Hazebroucq, S.; Labat, F.; Lincot, D.; Adamo, C. *J. Phys. Chem. A* **2008**, *112*, 7264.
(29) Joubert, L.; Guillemoles, J. F.; Adamo, C. *Chem. Phys. Lett.* **2003**, *371*, 378.
(30) Perpète, E.; Maurel, F.; Jacquemin, D. *J. Phys. Chem. A* **2007**, *111*, 5528.
(31) Preat, J.; Jacquemin, D.; Vercauteren, D.; Perpète, E. *Theor. Chem. Acc.* **2008**, *119*, 463.
(32) Persson, P.; Lundqvist, M. J.; Ernstorfer, R.; Goddard, W. A. III.; Willig, F. *J. Chem. Theory Comput.* **2006**, *2*, 441.
(33) Abuabara, S. G.; Rego, L. G. C.; Batista, V. S. *J. Am. Chem. Soc.* **2005**, *127*, 18234.
(34) Nilsing, M.; Persson, P.; Lunell, S.; Ojamäe, L. *J. Phys. Chem. C* **2007**, *111*, 12116.
(35) De Angelis, F.; Fantacci, S.; Selloni, A.; Grätzel, M.; Nazeeruddin, M. K. *Nano Lett.* **2007**, *7*, 3189.
(36) Nazeeruddin, M. K.; De Angelis, F.; Fantacci, S.; Selloni, A.; Viscardi, G.; Liska, P.; Ito, S.; Takeru, B.; Grätzel, M. *J. Am. Chem. Soc.* **2005**, *127*, 16835.
(37) Persson, P.; Lundqvist, M. J. *J. Phys. Chem. B* **2005**, *109*, 11918.
(38) Persson, P.; Lunell, S.; Brühwiler, P. A.; Schnadt, J.; Säodergren, S.; O'Shea, J. N.; Karis, O.; Siegbahn, H.; Martensson, N.; Bassler, M.; Patthey, L. *J. Chem. Phys.* **2000**, *112*, 3945.
(39) Lundqvist, M. J.; Nilsing, M.; Lunell, S.; Akermark, B.; Persson, P. *J. Phys. Chem. B* **2006**, *110*, 20513.
(40) (a) Ciofini, I.; Lainé, P. P.; Bedioui, F.; Adamo, C. *J. Am. Chem. Soc.* **2004**, *126*, 10763. (b) Lainé, P. P.; Loiseau, F.; Campagna, S.; Ciofini, I.; Adamo, C. *Inorg. Chem.* **2006**, *45*, 5538.
(41) Jacquemin, D.; Perpète, E. A.; Ciofini, I.; Adamo, C. *Acc. Chem. Res.* **2009**, *42*, 326.
(42) Labat, F.; Baranek, P.; Domain, C.; Minot, C.; Adamo, C. *J. Chem. Phys.* **2007**, *126*, 154703.
(43) Labat, F.; Baranek, P.; Adamo, C. *J. Chem. Theor. Comp.* **2008**, *4*, 341.
(44) Labat, F.; Adamo, C. *J. Phys. Chem. C* **2007**, *111*, 15034.
(45) Saunders, V. R.; Dovesi, R.; Roetti, C.; Orlando, R.; Zicovich-Wilson, C. M.; Harrison, N. M.; Doll, K.; Civalleri, B.; Bush, I.; D'Arco Ph.; Llunell, M. *Crystal 03 User's Manual*; Università di Torino: Torino, Italy, 2003.
(46) Adamo, C.; Barone, V. *J. Chem. Phys.* **1999**, *110*, 6158.
(47) Ernzerhof, M.; Scuseria, G. E. *J. Chem. Phys.* **1999**, *110*, 5029.
(48) Perdew, J. P.; Burke, K.; Ernzerhof, M. *Phys. Rev. Lett.* **1996**, *77*, 3865.
(49) Hay, P. J.; Wadt, W. R. *J. Chem. Phys.* **1985**, *82*, 270.
(50) Durand, P.; Barthelat, J.-C. *Theor. Chim. Acta* **1975**, *38*, 283.
(51) Barthelat, J.-C.; Durand, P. *Gazz. Chim. Ital.* **1978**, *108*, 225.
(52) Barthelat, J.-C.; Durand, P.; Serafini, A. *Mol. Phys.* **1977**, *33*, 159.
(53) Hay, P. J.; Wadt, W. R. *J. Chem. Phys.* **1985**, *82*, 284.
(54) Labat, F. ; Ciofini, I. ; Adamo, C. J. Chem. Phys., in press.
(55) Jaffe, J. E.; Harrison, N. M.; Hess, A. C. *Phys. Rev. B* **1994**, *49*, 11153.
(56) Zapol, P.; Jaffe, J. B.; Hess, A. C. *Surf. Sci.* **1999**, *422*, 1.
(57) Persson, P.; Ojamäe, L. *Chem. Phys. Lett.* **2000**, *321*, 302.

Structural optimizations have been carried out on the whole unit cell (EY/substrate), but the supercell relaxation has been restricted to the two outermost atomic planes, since surface relaxation of this substrate is known to mainly involve only the outermost atoms.[58] Standard parameters have been used for both geometry optimizations and for the evaluation of Coulomb and exchange series.[45]

Interaction energies were computed as the difference between the total energies of the combined adsorbate/substrate system and the ZnO surface plus an adsorbate molecule:

$$E_{\text{int}} = E_{\text{ads/sub}} - (E_{\text{sub}} + E_{\text{ads}}) \quad (1)$$

where $E_{\text{ads/sub}}$, E_{sub}, and E_{ads} correspond to the relaxed energies of the EY/ZnO supercell, the $2H^+$/ZnO supercell, and the isolated EY molecule, respectively. A negative value of E_{int} thus corresponds to a stable adsorption.[59]

UV−vis spectra have been simulated using the time dependent-DFT (TD-DFT) approach,[60] considering the same exchange-correlation functional and basis sets already described for periodic calculations. The convergence of the computed vertical transitions has been verified using the 6-31+G(d,p) basis set, which has been shown to provide reliable results for valence excitations.[61]

Environmental effects have been included in the TD-DFT calculations with two different approaches:

(1) To model the surface effects on the UV−visible absorption spectrum of EY, a QM:QM electronic embedding model,[62,63] based on the ONIOM scheme,[64] has been considered. In such an approach, the *high* computational level is obtained using the PBE0 functional with the above specified basis set, while the *low*-level is represented by the SVWN exchange-correlation functional[65] coupled with the LANL2 pseudopotentials and corresponding minimal basis sets.[66] In addition, the *real*-system low-level Mulliken charges define the embedding potential. The *model* system is represented by the EY molecule, while the *real* system, including both the EY molecule and the ZnO substrate, is modeled by a large hydrogen-saturated cluster (530 atoms) obtained from the optimized periodic structure (see Figure 3).

(2) In the second approach, solvent effects have been taken into account by an implicit approach, namely the polarizable continuum model (PCM),[67] using the nonequilibrium version of the IEF-PCM model,[68] water being considered as solvent.

All TD-DFT calculations have been carried out using a development version of the Gaussian program.[69]

To evaluate the electron injection time (τ, in fs) from the dye to the substrate, a model derived from the Newns−Anderson approach[70] has been considered. In this model, τ is estimated from

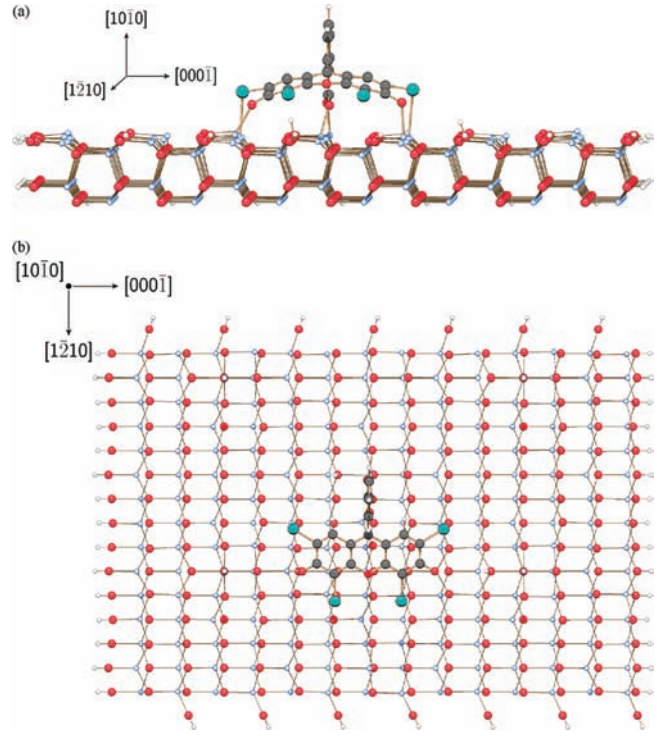

Figure 3. Side (a) and top (b) views of the 530-atoms cluster used for UV−vis spectra simulations: carbon, bromine, zinc, oxygen, and hydrogen atoms as black, cyan, red, light blue, and white balls, respectively.

the broadening (Δ, in meV) of the donor orbital of the dye upon adsorption, as

$$\tau = 658/\Delta \quad (2)$$

Such model, which has already been applied to numerous systems including dye/TiO_2 ones, typically provides estimates which are about one-half of the experimental ones,[32] in line with more sophisticated models.[71]

We stress that modeling of extended systems with limited models (clusters) could introduce spurious effects related to the finite-size of the models, thus leading to poor representation of the band structure, characterized by intruder states originating from the adsorbed molecule.[72] In this respect, periodic approaches have many advantages, as long as computational parameters such as the unit cell size and the slab thickness are carefully chosen. In particular, one way to assess the quality of the chosen periodic model is to verify that lateral interaction energies between ad-molecules are negligible with respect to the adsorbate/substrate interaction energy. The difference between the energy of an isolated adsorbate molecule, at its adsorbed geometry, and a monolayer of adsorbate molecules with the same periodicity as the interacting system allows estimating the intermolecular (lateral) interaction energy, directly related to the surface coverage. In our case, it is found to be less than 6% of the adsorbate/substrate interaction energy, with a computed value of 38 kJ/mol.

In addition, since an accurate description of the electronic structure of the interfacial dye/semiconductor is required, common local and gradient-corrected exchange-correlation functionals, which are well-known to significantly underestimate band gaps in solids due to the self-interaction problem,[73] should be avoided. To address

(58) Meyer, B.; Marx, D. *Phys. Rev. B* **2003**, *67*, 035403.
(59) Pisani, C. Loss of symmetry in crystals: surfaces and local defects. In Quantum-Mechanical ab-Initio Calculation of the Properties of Crystalline Materials; Pisani, C, Ed.; Lecture Notes in Chemistry; Springer-Verlag: Berlin, 1996; Vol. 67, pp 227-244.
(60) Stratmann, R. E.; Scuseria, G. E.; Frisch, M. J. *J. Chem. Phys.* **1998**, *109*, 8218.
(61) Ciofini, I.; Adamo, C. *J. Phys. Chem. A* **2007**, *111*, 5549.
(62) Hratchian, H. P.; Parandekar, P. V.; Raghavachari, K.; Frisch, M. J.; Vreven, T. *J. Chem. Phys.* **2008**, *128*, 034107.
(63) Jacquemin, D.; Perpéte, E. A.; Laurent, A. E.; Assfeld, X.; Adamo, C. *Phys. Chem. Chem. Phys.* **2009**, *11*, 1258.
(64) (a) Maseras, F.; Morokuma, K. *J. Comp. Chem,*. **1995**, *16*, 1170. (b) Humbel, S.; Sieber, S.; Morokuma, K. *J. Chem. Phys,*. **1996**, *105*, 1959.
(65) (a) Slater, J. C. *Quantum Theory of Molecular and Solids. Vol. 4: The Self-Consistent Field for Molecular and Solids* (McGraw-Hill, New York, 1974);(b) Vosko, S. H.; Wilk, L.; Nusair, M. *Can. J. Phys* **1980**, *58*, 1200.
(66) Hay, P. J.; Wadt, W. R. *J. Chem. Phys,*. **1985**, *82*, 270.
(67) Tomasi, J.; Mennucci, B.; Cammi, R. *Chem. Rev.* **2005**, *105*, 2999.
(68) Cossi, M.; Barone, V. *J. Chem. Phys.* **2001**, *115*, 4708.
(69) Frisch, M. J.; et al. *Gaussian GDV,* revision F.01; Gaussian, Inc.: Wallingford, CT, 2008.
(70) Newns, D. *Phys. Rev.* **1969**, *178*, 1123.
(71) Li, J.; Nilsing, M.; Kondov, I.; Wang, H.; Persson, P.; Lunell, S.; Thoss, M. *J. Phys. Chem. C* **2008**, *112*, 12326.
(72) Minot, C.; Markovits, A. *J. Mol. Str. (THEOCHEM)* **1998**, *424*, 119.
(73) Corà, F.; Alfredsson, M.; Mallia, G.; Middlemiss, D. S.; Mackrodt, W. C.; Dovesi, R.; Orlando, R. *Struct. Bonding (Berlin)* **2004**, *113*, 171.

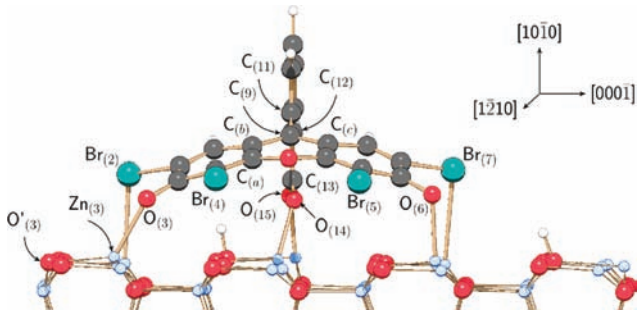

Figure 4. Side view of the adsorption mode of EY on ZnO wurtzite (10−10).

this issue, one of the possibilities is to consider hybrid HF/DFT schemes with the so-called hybrid functionals, which have been found to give a very accurate description of the electronic structures of solids.[74] In particular, band gaps are accurate within 0.3 eV for typical semiconductor materials, when the PBE0 functional is used.[42−44,75] Furthermore, since this latter functional has also been found particularly suitable for the modeling of the UV−visible spectra of dyes, both in gas phase and in solution, our overall computational setup allows for a correct and coherent (i.e., on an equal footing) description of all components and processes taking place in hybrid DSSC. However, as long as investigated properties are local, as it is the case for electronic excitations of the dye, cluster approximations represent a viable alternative to periodic model.

3. Results and Discussion

In the following EY denotes the fully deprotonated dianionic eosine-Y molecule since this is the form that adsorbs on the surface through its carboxylate group at the experimental pH. Thus, all geometrical and electronic features, including the UV−vis spectra, of EY both when isolated and adsorbed on ZnO, refer to this deprotonated dianionic molecule. Indeed, to deal with a neutral supercell the two acidic protons were adsorbed on the most nucleophilic oxygen sites of the surface. Thus, the EY/ZnO periodic system is constituted by EY (dianionic) adsorbed on the surface and two protons adsorbed on the same supercell.

3.1. Structural and Energetic Features. For molecules possessing a carboxylate group, three main adsorption modes on a metal oxide surface can generally be considered: bridging, unidentate, and chelate. The first one, which was proven to be the most stable by far, both at experimental[76] and theoretical[54,77] levels in the case of ZnO, shows two oxygen atoms pointing toward two different metal atoms. In the following, therefore, only this adsorption model (bridging) will be considered for the adsorption of EY on the ZnO (10−10) substrate, which is the most stable ZnO orientation.[78]

Figure 4 reports the optimized structure of the EY adsorbed on the ZnO wurtzite (10−10) substrate, corresponding selected parameters being given in Supporting Information (Table S1). If in both cases, the xanthenes and phenyl moieties are practically orthogonal, few but significant modifications can be noticed upon adsorption. In particular, the carboxylate moiety twists, as evidenced by the increasing of the $O_{(14)}C_{(13)}C_{(12)}C_{(11)}$ dihedral angle (from 0° to −5°) and by the value of the dihedral angle formed by the oxygen and zinc atoms which is significantly different from zero ($Zn_{(14)}O_{(14)}O_{(15)}Zn_{(15)}$, −21.9°). Such structural rearrangements, along with the lengthening of the CO bonds and the large outward relaxation of the Zn atoms toward EY (+0.30 Å, see Table S2), suggest a donation/back-donation interaction mechanism between oxygen and zinc atoms.

The xanthene moiety also undergoes important structural modifications. In particular, upon adsorption, the EY molecule bends toward the surface through its xanthene moiety, as can be clearly seen from Figure 4 and from the dihedral angles reported in Table S2. Indeed, additional interactions involving two Zn−O bonds ($O_{(6)}Zn_{(6)}$ and $O_{(3)}Zn_{(3)}$, 2.115 and 2.124 Å, respectively) and two Zn−Br bonds ($Br_{(7)}Zn_{(7)}$ and $Br_{(2)}Zn_{(2)}$, 3.036 and 2.868 Å, respectively) can be evidenced. The Zn−O distances are not far from those involving the oxygen atoms of the benzoate moiety (2.067 and 2.016 Å), thus suggesting a strong adsorbate/substrate interaction. In turn, the corresponding carbonyl bonds, $CO_{(6)}$ and $CO_{(3)}$, increase from 1.241 Å in the isolated case to more than 1.265 Å in the adsorbed case. Finally, we note that the $CBr_{(7)}$ and $CBr_{(2)}$ bonds are slightly shorter in the adsorbed case than in the isolated one, and nearly parallel to the ZnO surface.

These geometrical variations, as well as the significant modification of the charge patterns (see below), suggest a strong interaction between the adsorbate molecule and the surface. A significantly different behavior of the xanthene and benzoate moieties of the EY molecule can thus be easily evidenced upon adsorption. From one side the adsorption mainly involves the anchoring carboxylate moiety of the latter, while, on the other side, the former is strongly bent in order to maximize its interactions with the ZnO substrate. Four new interactions of the adsorbate with the substrate can indeed be highlighted, two Zn−O and two Zn−Br ones, in line with the experimentally suggested interaction of the xanthene O atoms with the substrate.[78]

Furthermore, as can be evidenced from Table S2, the adsorption also induces significant modifications of the substrate along the [0001] and [10−10] directions, while the displacements along the [1−201] direction are very low (less than 0.05 Å). Large displacements occur in order to both maximize the adsorbate/substrate interaction and minimize the substrate reorganization, while maintaining its typical dimer-stacked pattern. Nevertheless, the four newly created interactions of the adsorbed EY molecule involving its xanthene moiety lead to significant atomic displacements of the outermost surface atoms with, for instance, large computed displacements for the $Zn_{(15)}$ and $Zn_{(14)}$ atoms along [10−10] and [0001]. Consequently, the computed interaction energy is significant.[59,79]

3.2. Electronic Features of the EY/ZnO Assembly. An efficient dye/substrate assembly for DSSC applications is normally characterized by a highest occupied molecular orbital (HOMO) level, corresponding to that of the isolated dye, lying energetically in the band gap region of the semiconductor. Although its energy may be shifted when the sensitizer is adsorbed on the surface, its electronic interaction with the substrate is supposed to be weak, thus to be considered as a small perturbation. This level should therefore be readily identifiable as a single molecular level with a negligible broadening, even in the aggregate. The lowest unoccupied molecular orbital (LUMO) of the isolated dye on the other hand, which is the donating orbital involved in the electron injection, is expected

(74) Corà, F. *Mol. Phys.* **2005**, *103*, 2483.
(75) Franchini, C.; Bayer, V.; Podloucky, R.; Paier, J.; Kresse, G. *Phys. Rev. B* **2005**, *72*, 045132.
(76) (a) Davis, R.; Walsh, J. F.; Muryn, C. A.; Thornton, G.; Dhanak, V. R.; Prince, K. C. *Surf. Sci. Lett.* **1993**, *298*, L196. (b) Crook, S.; Dhariwal, H.; Thornton, G. *Surf. Sci.* **1997**, *382*, 19.
(77) Persson, P.; Lunell, S.; Ojamäe, L. *Int. J. Quantum Chem.* **2002**, *89*, 172.
(78) Hilgendorff, M.; Sundstrom, V. *J. Phys. Chem. B* **1998**, *102*, 10505.

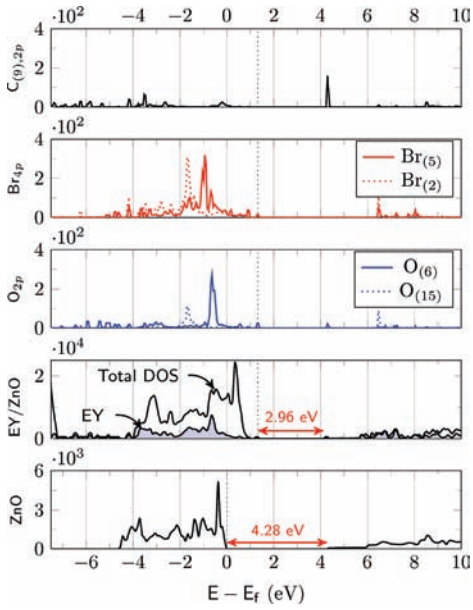

Figure 5. Total and projected densities of states of EY adsorbed on ZnO wurtzite (10−10). From top to bottom: projection onto the 2p orbitals of the adsorbate $C_{(9)}$ atom; projections onto 4p orbitals of the adsorbate Br atoms (solid lines, $Br_{(5)}$ contribution; dotted lines, $Br_{(2)}$ contribution); projections onto 2p orbitals of the adsorbate O atoms (solid lines, $O_{(6)}$ contribution; dotted lines, $O_{(15)}$ contribution); total eosin contribution (filled curve) to the total DOS scaled by a factor of 2; clean surface DOS (scaled by a factor of 10). The Fermi level (E_f) of the clean surface is set to 0 eV in all cases. Atom labeling corresponds to that of Figure 2.

to interact significantly with the conduction band of the semiconductor, giving a number of mixed sensitizer-semiconductor levels upon adsorption.

A clear-cut vision of the electronic structure as well as of the photoinduced electron transfer (ET) process in dye-loaded semiconductor thin films can be obtained combining a detailed density of states (DOS) and projected DOS (PDOS) analysis to plotting of relevant Γ-point orbitals. In Figures 5 and 6, such data are represented. As can be noticed from Figure 5, the adsorbate EY molecule contributes largely to the density of states of the combined EY/ZnO system over a broad energy range, both in the valence band (VB) and the conduction band (CB), thus suggesting a significant interaction between the adsorbate and the substrate, in line with the previously given geometric and energetic analysis. Such interaction results in a decrease of the computed band gap from 4.28 eV for the clean surface to 2.96 eV upon EY adsorption. In fact, both the bottom of the CB and the top of the VB originate from adsorbate states. Indeed, as pointed out by Figure 6, the Γ-point HOMO is mainly composed of 2p contributions of the C, Br, and O atoms of the xanthene moiety of EY while the LUMO is built up from 2p orbitals of this latter moiety, with major contributions arising from $C_{(7)}$, whose $2p_z$ orbital has an antibonding interaction with the xanthene π orbitals. In other words both HOMO and LUMO retain their molecular character. Such features are in clear contrast with those observed in other DSSC assemblies, where the LUMO has the character of a semiconductor CB state, with the sensitizer virtual orbital overlapping with the bottom of the CB.[35,80] This typical interaction can only be evidenced at higher energy, the LUMO + 1 crystalline orbital possessing a mixed adsorbate/substrate character, deriving mainly from a combination of Zn 4s and O 2s substrate orbitals with the xanthene $C_{(7)}$ $2p_z$ orbital. The LUMO + 2 crystalline orbital on the other hand, is exclusively localized on the ZnO substrate, displaying only contributions of Zn 4s orbitals.

In the case of a symmetric adsorption on both surfaces of the slab, the same picture holds but two degenerate HOMOs (localized one of each EY) and LUMOs (also localized one of each EY) are found, the first unoccupied orbital with predominant ZnO contributions being the LUMO + 2 (refer to Figure S1 in Supporting Information) thus validating the model used.

As could be expected, states originating from the carboxylate groups of the benzoate moiety occur at much lower energies, pointing out that anchor groups cannot contribute to the photoexcitation phenomena, as already reported for isolated dyes.[24,26] Indeed, as can be evidenced from Figure 5, benzoate oxygen atom ($O_{(15)}$) 2p orbitals contribute to lower energies than xanthene $O_{(6)}$ 2p orbitals. In addition, bonding between the $Br_{(7)}$ ($Br_{(2)}$) and $Zn_{(7)}$ ($Zn_{(2)}$) atoms results in a shift of the $Br_{(7)}$ and $Br_{(2)}$ contributions to lower energies, when compared to the two other Br contributions, namely $Br_{(5)}$ and $Br_{(4)}$.

Electronically, these effects are reflected on the computed Mulliken charges for the isolated and adsorbed species (Table 1), suggesting a significant charge transfer between the adsorbate and the substrate. This is well summarized by the adsorbate (EY) overall charge which decreases from −2.00 |e⁻| to −1.31 |e⁻| upon adsorption, a variation of +0.69 |e⁻|. This significant charge loss is mainly shared between both the four bromine atoms (+0.48 |e⁻|), showing each an average +0.12 |e⁻| increase, and the xanthene atoms (+0.22 |e⁻|).

No significant difference ($\Delta < 0.01$ |e⁻|) in computed charges is found when using a symmetrized slab model.

3.3. Modeling of the UV−Visible Spectra. Like many other members of the xanthene family, the absorption properties of eosin-Y are experimentally well-known. In particular, its absorption spectrum is strongly pH-dependent due to protonation of oxygen atoms, either in the benzoate or the xanthene moieties.[81] Furthermore, a highly pH-dependent tautomeric equilibrium between the quinoidal and lactone forms can also be envisaged for this molecule.[82] Nevertheless, since the pK_a value of EY in water is 5.0[83] and since the ZnO/EY hybrid films are prepared at a local pH of 10.5,[12] in the following, we only focus on the deprotonated species (EY).

Computed vertical transitions, as well as simulated UV−vis spectra for all species and models investigated are reported in Table 2 and Figure 7, respectively.

We can first note that, for all species and models, in the energy range investigated, two bands can be clearly evidenced, in agreement with experimental data.[84−86]

For the isolated dye, at its optimized gas phase geometry, the first band centered at 432 nm is the most intense ($f = 0.53$) and corresponds to a $\pi \rightarrow \pi^*$ transition between the HOMO and the LUMO. The second is an $n \rightarrow \pi^*$ transition, centered at 391 nm and less intense ($f = 0.18$), between the HOMO − 1 and the LUMO, the first being mainly centered on the oxygen atoms

(79) The computed interaction energy of EY with ZnO (10−10) is−653 kJ/mol.

(80) Duncan, W. R.; Prezhdo, O. V. *J. Am. Chem. Soc.* **2008**, *130*, 9756.
(81) Abe, R.; Hara, K.; Sayama, K.; Domen, K.; Arakawa, H. *J. Photochem. Photobiol. A* **2000**, *137*, 63.
(82) Mchedlov-Petrossyan, N. O.; Kukhtik, V. I.; Bezugliy, V. D. *J. Phys. Org. Chem.* **2003**, *16*, 380.
(83) Levitan, H. *Proc. Natl. Acad. Sci. U.S.A.* **1977**, *74*, 2914.
(84) Birla, L.; Cristian, A. M.; Hillebrand, M. *Spectrochim. Acta A* **2004**, 6–551.
(85) Gratz, H.; Penzkofer, A. *J. Photochem. Photobiol. A* **1999**, *127*, 21.
(86) Fink, D. W.; Willis, C. R. *J. Chem. Phys.* **1970**, *53*, 4720.

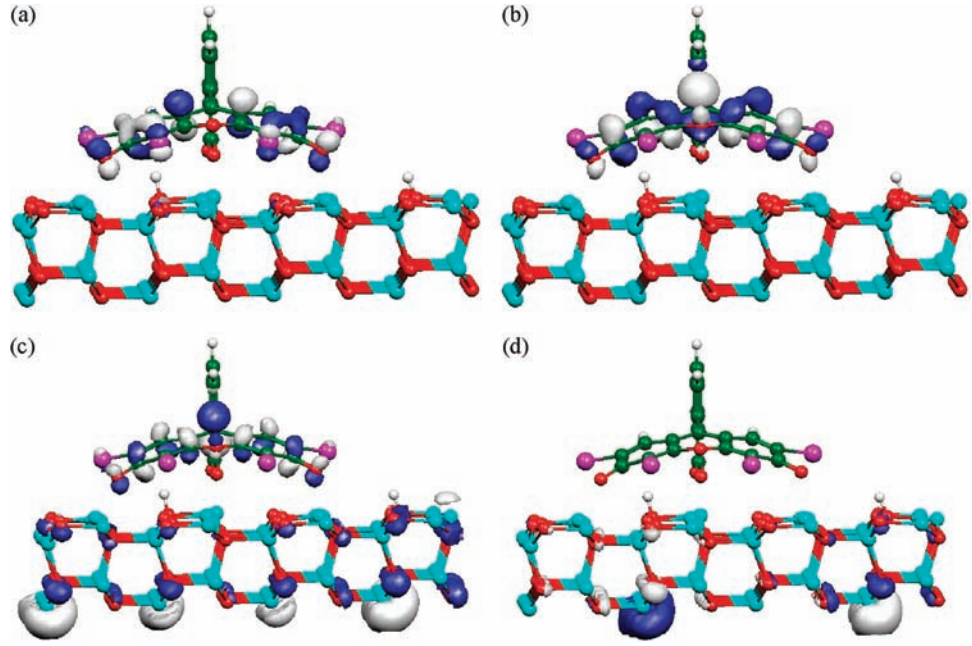

Figure 6. Γ-point computed (a) HOMO, (b) LUMO, (c) LUMO + 1, and (d) LUMO + 2 crystalline orbitals of EY/ZnO. Isovalues: 0.040, 0.030, 0.015, and 0.020 au, respectively.

Table 1. Mulliken Atomic Charges (in |e⁻|) of Both Isolated and Adsorbed Eosin. Labeling Corresponds to That of Figure 4

atoms	isolated	adsorbed
$Zn_{(14)}/O_{(14)}$	+0.969/−0.585	+1.061/−0.552
$Zn_{(15)}/O_{(15)}$	+0.969/−0.628	+1.078/−0.608
$Zn_{(10)}/O_{(10)}$	+0.969/−0.539	+1.041/−0.606
$Zn_{(3)}/O_{(3)}$	+0.969/−0.539	+1.087/−0.597
$Zn_{(7)}/Br_{(7)}$	+0.969/−0.539	+0.982/+0.100
$Zn_{(2)}/Br_{(2)}$	+0.969/−0.020	+0.961/+0.126
EY[a]	−2.000	−1.300

[a] Total charge on EY.

Table 2. Wavelengths of the Main Vertical Transitions (λ, nm) and Corresponding Oscillator Strengths (f) Computed for EY, both in Gas Phase and Solution Considering Different Geometries and Environments. Only Transitions with Oscillator Strengths Greater than 0.10 Are Reported

geometry	environment	λ	assignment	f
bare	isolated	432	$\pi\rightarrow\pi^*$	0.53
		391	$n\rightarrow\pi^*$	0.18
solution	solution	439	$\pi\rightarrow\pi^*$	0.85
		395	$\pi\rightarrow\pi^*$	0.11
adsorbed	isolated	454	$\pi\rightarrow\pi^*$	0.21
		415	$\pi\rightarrow\pi^*$	0.47
adsorbed	surface	452	$\pi\rightarrow\pi^*$	0.35
		408	$\pi\rightarrow\pi^*$	0.15

of the carboxylate group. It is interesting to note that the calculated HOMO/LUMO and HOMO − 1/LUMO gaps are 415 and 387 nm, respectively, thus outlining the intrinsic one-electron nature of the aforementioned transitions. For both of these, band maximum positions are shifted by about 80 nm with respect to the experimental data. In fact, the UV spectrum of the native dianion form of EY has been experimentally recorded and it shows one intense band at 516 nm, with a shoulder around 480 nm, both transitions being recorded either in water (at pH 7.4) or in methanol.[84,85] This difference is slightly larger than expected for the level of theory used[41] but close to previous results.[28]

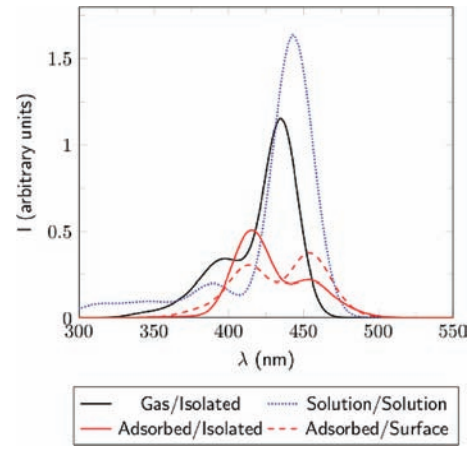

Figure 7. UV−vis absorption spectra of EY in different environments. All spectra have been simulated by associating a single Gaussian function with a half-height width of 0.15 eV to each computed transition.

Solvent affects both bands. As could be expected, while the first band is only slightly red-shifted (+7 nm) and increases in intensity, a much larger solvent effect is computed for the $n\rightarrow\pi^*$ transition, with a blue-shift of −24 nm and a significant oscillator strength decrease (from 0.18 to 0.002). Interestingly, a new band corresponding to multiple $\pi\rightarrow\pi^*$ transitions centered at 395 nm grows in intensity when compared to the isolated case.

A much pronounced effect on UV−visible spectra is computed when taking account of adsorption on the surface. Indeed, not only are the two $\pi\rightarrow\pi^*$ transition energies both red-shifted by about +20 nm (to 452 and 408 nm, respectively) but their oscillator strengths are also significantly affected, with an inversion of their relative intensities with respect to the isolated dye (see Table 2 and Figure 7). It must be noted that the experimental spectrum of EY on ZnO film is indeed characterized by two peaks very close in intensity, centered around 500 and 525 nm.[8b]

Since the natures of the orbitals involved in the transitions are not affected upon adsorption, the calculated red-shift can be related to a geometrical effect, that is the bending of the xanthene moiety toward the ZnO surface. To further clarify this point, additional calculations have been carried out for the isolated molecule at its adsorbed geometry (see Table 2 and Figure 7). Computed transition energies are only slightly different from those obtained when taking into account the surface environment, a maximal deviation of 7 nm being calculated, thus confirming the dominant structural effect.

To sum up, from our calculations, the adsorption properties of the dye are significantly modified by the interaction with the semiconductor surface, both in terms of transition energies and intensities (oscillator strengths). Nevertheless, we should stress that the spectral signature of EY is globally preserved, thus confirming that in silico isolated dye design is possible to enhance DSSC performances.

3.4. Simulation of the Electron Injection. Electron injection in the most common DSSC takes place on a femtosecond time scale,[87] thus showing that there is sufficiently strong electronic coupling between substrate and adsorbate for the ET to proceed faster than the nuclear relaxations as well as other competing processes.[5] Experimental data indicate that DSSC efficiency is indeed independent from the temperature and that the initial ET is constant over a significant temperature range.[88] Theoretical simulation of the electron injection from the dye into the conduction band of the semiconductor could give some insights to the main features of such a process. Furthermore, first principles dynamic simulations on model systems have confirmed that this ET process is dominated by an adiabatic mechanism.[33,80]

A simplified, yet informative, way to investigate processes occurring from an excited state of a system is via analysis of the reduced species, obtained by adding one (or more) electrons to the adsorbed EY/ZnO system as a suitable model of the excited state of the native system. Such an approach is analogous to experimental spectro-electrochemical studies used to mimic excited states resulting from photoinduced electron transfer processes such as charge-separated or even charge transfer states, which are otherwise difficult to identify and characterize due to their short lifetimes.[40] Furthermore, hybrid DFT approaches, such as the one here used, have recently been shown to be particularly suitable for dealing with reduced periodic systems.[89]

Analysis of the electronic properties of the obtained reduced system can be carried out looking at the spin density, that is the difference between the α-electron and the β-electron densities. Such densities, computed for both mono- and bireduced EY/ZnO systems, are reported in Figure 8. As can be clearly seen, spin densities of the monoreduced EY/ZnO system are mainly localized on the xanthene moiety of EY, the substrate fragment contributing to only 30% of the total α spin density, suggesting an unfavorable injection of the first excited electron from the adsorbate to the substrate. This is of course related to a Γ-point LUMO crystalline orbital strictly localized on the EY molecule. In contrast, in the N3/TiO_2 system, the TiO_2 substrate

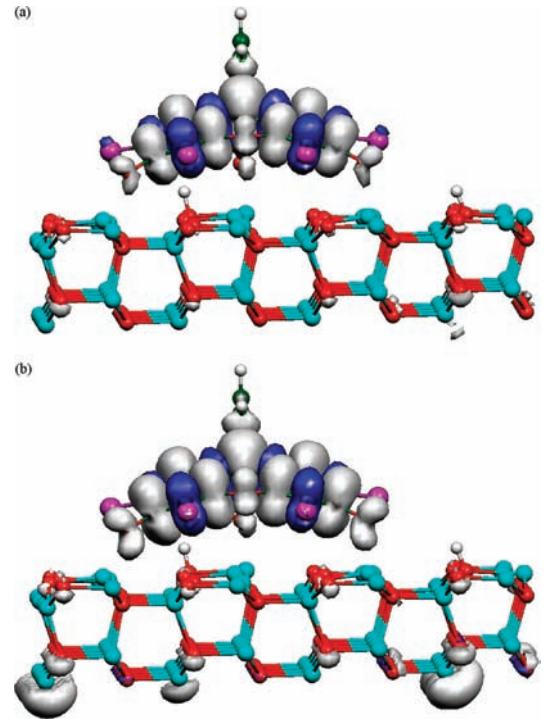

Figure 8. Γ-point computed spin densities of the reduced EY/ZnO system: (a) monoreduced specie; (b) bireduced specie. Isovalue: 0.0005 au.

contributes to 100% of the total α spin density of the monoreduced system.[90]

Adding a second electron onto the EY however reveals that the computed spin densities are spread over both the substrate and the adsorbate, with a 48% contribution to the total α spin density originating from the substrate (see Figure 6).

The same conclusions hold when using a symmetric slab model (one EY on each side) although in this case it is necessary to inject two electrons (one per EY) before reaching a direct injection to ZnO (with the third electron) as can be easily seen from the computed spin density for this system when reduced one, two, or three times (Figure S2).

From our calculations therefore, in order to effectively inject one electron (that is, 48% of two electrons) from the adsorbate to the ZnO substrate, two electrons are mobilized (including one from a remote donor) and absorption of two photons by the EY/ZnO system is required. The point, here, is that an intervening electron donor does not come into play to regenerate the oxidized dye subsequent to electroinjection into the semiconductor but rather reacts with the primary photoexcited dye prior to final electron injection triggered by a second photon. In other words, an injection from the LUMO + 1 seems to prevail in a such system, in line with the much slower injection times experimentally observed for the N3/ZnO system compared to the N3/TiO_2 one (100 ps and 50 fs, respectively[91]). It is also noteworthy that the ratio of the previously mentioned substrate contributions to the summed monoreduced α spin density in both the N3/TiO_2 and EY/ZnO cases (3.3), is close to that of their conversion efficiencies (4.8), suggesting that the large

(87) Tachibana, Y.; Moser, J. E.; Grätzel, Klug, D. R.; Durrant, J. R. *J. Phys. Chem.* **1996**, *100*, 20056.
(88) Grätzel, M. *J. Photochem. Photobiol. C: Photochem. Rev.* **2003**, *4*, 145.
(89) Finazzi, E.; Di Valentin, C.; Pacchioni, G.; Selloni, A. J. *Chem. Phys.* **2008**, *129*, 154113.
(90) Calculations of N3 on the anatase TiO_2 (101) were performed using the same level of theory here applied (that is PBE0) using a periodic supercell containing a total of 239 atoms. Such cell corresponds to the experimental coverage of 0.3 molecules/nm^2.
(91) Asbury, J. B.; Hao, E.; Wang, Y.; Ghosh, H. N.; Lian, T. *J. Phys. Chem. B* **2001**, *105*, 4545.

difference between these two systems in injection times and conversion efficiencies, can be attributed to different number of photons involved in the injection process at the dye/semiconductor interface. This is in line with a recent experimental work, suggesting a bielectronic process for the reduction of the EY/Zn(II) system.[92]

A significant enhancement of the EY/ZnO DSSC system could thus be obtained by reduction of the dye by a remote electron donor (preferably covalently linked to the dye so as to overcome diffusion limited effects) since it appears as a typical example of the so-called "injection from the reduced sensitizer" mechanism (see Figure 1b).[93,94] In this mechanism, the dye excited state is first quenched by an external donor (D in Figure 1) and then transfers the hot electron to the semiconductor. The net result is a global bielectronic injection process from the dye to the semiconductor. Such a mechanism has already been reported in experimental studies of several ruthenium polypyridyl dyes, using phenothiazine as reducing agent in some cases.[94]

To better characterize the efficiency of the reduced EY/ZnO system, the injection time from the reduced dye to ZnO has been computed and compared to values obtained for two reference systems for which experimental data are available: N3/TiO_2 and BINA/TiO_2 (BINA refers to bi-isonicotinic acid, the surface anchoring ligand involved in N3). Results obtained indicate that the injection time is 8 fs in EY/ZnO]$^-$, 22 fs in N3/TiO_2 (exptl, ~50 fs[90]) and 2 fs in BINA/TiO_2 (exptl, < 3 fs[95]). From our calculations therefore, the injection time is about 3 times shorter (i.e., faster injection) in EY/ZnO]$^-$ than in the standard N3/TiO_2 cell.

4. Conclusions

The adsorption of eosin-Y on the ZnO wurtzite (10−10) substrate has been investigated using hybrid DFT techniques within a periodic approach, considering only the most stable adsorption mode previously characterized for the formic acid model system:[54] a bridging dissociative mode in benzoate. The EY/ZnO system has been fully characterized at the geometric, energetic, and electronic levels. To check the feasibility of an electron transfer from the adsorbate to the substrate, reduced EY/ZnO systems obtained by artificially adding electrons to the neutral system, have been considered. Electronic structure investigations included densities of states calculations, Γ-point computed frontier crystalline orbitals, and spin densities analysis.

The main conclusions of this paper can be summarized as follows:

(1) EY firmly adsorbs on ZnO (10−10), both through its benzoate and xanthene moieties. This latter strongly distorts upon adsorption, to accommodate a bonding interaction with the substrate involving both Br and O atoms. The two EY subunits are flexible enough to favor the interactions, but internal geometric modifications of EY remain small. As a consequence, the UV−visible spectral signature of the isolated EY molecule is still found when adsorbed on ZnO, though slightly red-shifted.

(2) Both the HOMO and the LUMO of EY lie within the ZnO (10−10) band gap and are exclusively localized on the dye. Thus, direct HOMO→LUMO excitation does not lead to electron injection into the semiconductor. Only when an electron is injected in the LUMO + 1 level, the first unoccupied orbital with contributions from the ZnO, can a direct injection take place.

(3) A two electron mechanism is proposed to rationalize the low efficiency of the EY/ZnO solar cells.

As a consequence, two different strategies are proposed to enhance the cell efficiency. The first one rests on the addition of a remote (eventually external) electron-donating group (reducing agent). The second is based on chemical modifications of the dye, aimed at tuning the LUMO position in order to bring it above the CB bottom, which might result in direct injection process as in the N3/TiO_2 case.[89] Work is in progress in our laboratory to further investigate both strategies. In particular, aiming at the design of new dyes, we propose a strategy based on an *in silico* prescreening of spectral features on the isolated dyes combined with a comparison of the computed HOMO/LUMO energies with the computed edges of the valence and conduction bands. Indeed, preliminary results obtained have demonstrated that the choice of the anchoring group, although completely transparent from the point of view of the spectral properties, can be of crucial importance for a rational design of the dye/semiconductor interactions.

Acknowledgment. D. Lincot, T. Pauporté, and T. Le Bahers (ENSCP, Paris) are thanked for very stimulating discussion and useful experimental information on the EY-based DSSC. The French Super-Computer Center, CINES, is acknowledged for a generous amount of computer time (project 6064). I.C. thanks the French National Agency for Research (ANR) for financial support in the framework of the program 2008 "Habitat intelligent et solaire Photovoltaïque ≫ (Habisol) project ASYSCOL (Approche systémique de cellules solaires à colorant à base de ZnO). K.R. acknowledges support from the National Science Foundation (Grant NSF-0616737 and NSF-0911454).

Supporting Information Available: Complete ref 69; structural parameters of isolated and adsorbed EY; displacements of outermost substrate atoms; additional figures. This material is available free of charge via the Internet at http://pubs.acs.org.

JA902833S

(92) Goux, A.; Pauporté, T.; Lincot, D.; Dunsch, L. *Chem. Phys. Chem.* **2007**, *8*, 926.
(93) Watson, D. F.; Meyer, G. J. *Annu. Rev. Phys. Chem.* **2005**, *56*, 119.
(94) Thompson, D. W.; Kelly, C. A.; Farzad, F.; Meyer, G. J. *Langmuir* **1999**, *15*, 650.
(95) Schnadt, J.; Brühwiler, P. A.; Patthey, L.; O'Shea, J. N.; Södergreen, S.; Odelius, M.; Ahuja, R.; Karis, O.; Bässler, M.; Persson, P.; Siegbahn, H.; Lunell, S. *Nature* **2002**, *418*, 620.